

15. Luizão, R. C. C. *et al.*, Variation of carbon and nitrogen cycling processes along a topographic gradient in a central Amazonian forest. *Global Change Biol.*, 2004, **10**, 592–600.
16. Aerts, R., Nutrient resorption from senescing leaves of perennials: Are there general patterns? *J. Ecol.*, 1996, **84**, 597–608.
17. Wright, I. J. and Cannon, K., Relationships between leaf lifespan and structural defences in a low nutrient, sclerophyll flora. *Funct. Ecol.*, 2001, **15**, 351–359.
18. Wright, S. J., Seasonal drought, soil fertility and the species density of tropical forest plant communities. *Trends Ecol. Evol.*, 1992, **7**, 260–263.
19. Austin, A. T. and Vitousek, P. M., Precipitation, decomposition and litter decomposability of *Metrosideros polymorpha* in native forests on Hawaii. *J. Ecol.*, 2000, **88**, 129–138.
20. Coley, P. D., Herbivory and defensive characteristics of tree species in a lowland tropical forest. *Ecol. Monogr.*, 1983, **53**, 209–233.
21. Wardle, D. A., Bonner, K. I. and Barker, G. M., Linkages between plant litter decomposition, litter quality and vegetation responses to herbivores. *Funct. Ecol.*, 2002, **16**, 585–595.
22. Berg, B. and McLaugherty, C., Nitrogen release from litter in relation to the disappearance of lignin. *Biogeochemistry*, 1987, **4**, 219–224.

ACKNOWLEDGEMENTS. We thank UGC–CSIR, India for financial assistance through Research Fellowship programme (JRF/SRF–NET) and Kerala Forest and Wild Life Department for permission; We also thank Tana E. Wood, University of Virginia, USA for review comments and K. T. Thomachan, Devagiri College, Calicut for statistical analysis.

Received 23 August 2006; revised accepted 6 March 2007

Fundamental mass ratio relationships of whole-rock chondritic major elements: Implications on ordinary chondrite formation and on planet Mercury's composition

J. Marvin Herndon

Transdyne Corporation, 11044 Red Rock Drive, San Diego, California 92131, USA

The high occurrence on earth of ordinary chondritic meteorites and the making of models based upon assumptions has led to some confusion about the origin of ordinary chondrites and their role in planet formation. Major element fractionation among chondrites has been discussed for decades as ratios relative to Si or Mg. Expressing ratios relative to Fe leads to a new relationship admitting the possibility that ordinary chondrite meteorites are derived from two components: one is a relatively undifferentiated, primitive component, oxidized like the CI or C1 chondrites; the other is a

somewhat differentiated, planetary component, with oxidation state like the reduced enstatite chondrites. Such a picture would seem to explain for the ordinary chondrites, their major element compositions, their intermediate states of oxidation, and their ubiquitous deficiencies of refractory siderophile elements. I suggest that the planetary component of ordinary chondrite formation consists of planet Mercury's missing complement of elements, presumably separated from protoplanetary Mercury during its formation.

Keywords: Asteroid, element fractionation, mercury, meteorite formation, ordinary chondrite.

DIFFERENCES in mean densities of the terrestrial planets have long been interpreted as implying differences in the major element compositions of the inner planets. As first noted by Urey¹, the planet Mercury consists mainly of iron; at some point during the formation of Mercury, a significant portion of the silicate-forming elements, originally associated with that mass of iron was lost^{2,3}. Although various mechanisms have been proposed to account for the high density of Mercury⁴, the ultimate fate of its complement of lost elements, what became of them, has not, to my knowledge, been addressed.

The constancy in isotopic compositions of most of the elements of the earth, the moon, and the meteorites indicates formation from primordial matter of common origin. Primordial elemental composition is yet manifest and determinable to a great extent in the outermost regions of the sun. The less volatile rock-forming elements, present in the outer regions of the sun, occur in nearly the same relative proportions as in chondritic meteorites. For more than a century, chondrite compositions have been considered relevant to the bulk compositions of the terrestrial planets^{5–8}. But chondrites differ from one another in their respective proportions of major elements^{9,10}, in their states of oxidation^{11,12}, mineral assemblages¹³, and oxygen isotopic compositions¹⁴ and, accordingly, are grouped into three distinct classes: enstatite, carbonaceous and ordinary. Understanding how these three distinct classes originated and how they are related to the compositions of planets are among the most fundamental problems in solar system science.

The ordinary chondrites comprise 80% of the meteorites that are observed falling to the earth. Last century, during the 1970s, the widely cited 'equilibrium condensation model' was predicated on the assumption that minerals characteristic of ordinary chondrites formed as condensate from a gas of solar composition¹⁵. However, Herndon and Suess¹⁶ demonstrated from thermodynamic considerations that the oxidized iron content of the silicates of ordinary chondrites was consistent instead, with their formation from a gas phase depleted in hydrogen by a factor of about 1000 relative to solar composition. Subsequently, the present author¹⁷ showed that if the mineral assemblage characteristic of ordinary chondrites

e-mail: mherndon@san.rr.com

could exist in equilibrium with a gas of solar composition, it was at most only at a single low temperature, if at all. Moreover, oxygen depletion, relative to solar matter was also required, as might be expected from the re-evaporation of condensed matter after separation from solar gases.

For the past 15 years or so, concomitant with the development of micro-analytical techniques, there has been a marked disinterest in making systematic whole-rock analyses of chondrites. Instead, advances in micro-analytical capability have led to increasing focus on individual chondrite grains¹⁸. Such micro-analytical studies, for example, Marhas and Goswami¹⁹, provide a plethora of rich and diverse detail. The present communication, rather than focusing upon mineralogical detail, is based entirely on whole-rock analytical data expressed as ratios.

The abundances of elements in chondrites are expressed in the literature as ratios, usually relative to silicon (E_i/Si) and occasionally relative to magnesium (E_i/Mg). Expressing the Fe–Mg–Si elemental abundances as ratios relative to iron (E_i/Fe) leads to a relationship bearing on the origin of ordinary chondrites. This relationship admits the possibility that each ordinary chondrite consists in the main of a mixture of matter from two distinct and reasonably well-characterized reservoirs. The relationship obtained suggests the possibility that the complement of lost elements of Mercury may comprise one of the two components from which ordinary chondrites appear to have been derived.

Only three major rock-forming elements, iron, magnesium and silicon, together with combined oxygen and sulphur, account for at least 95% of the mass of each anhydrous chondrite and, by implication, each of the terrestrial planets. Figure 1 presents published analytical whole-rock Fe–Mg–Si data for 206 chondrites, expressed as molar (atom) ratios with respect to iron (Mg/Fe vs Si/Fe). Major element data for chondrites appear in Figure 1 to scatter about three distinct, least squares fit, straight lines when plotted as three separate datasets based upon major chondrite classes. The three well-defined straight lines, indicated by dashes in Figure 1, arise as a result of expressing ratios relative to Fe; chondrite data expressed as ratios relative to Si or Mg, in the usual manner, will not yield three well-defined straight lines, as shown in Table 1.

The existence of three well-defined straight lines for the three sets of chondrite data (Figure 1) is evident visually (note the expanded detail of the inset) and is demonstrated statistically both by the squares of the correlation coefficients and by the standard error of the least squares regression lines. The standard errors of estimate, calculated for each of the least squares fit straight lines, are shown in Figure 1 only in the two regions of intersection of the lines. Intersections of the standard errors of the respective least squares regression lines inscribe parallelograms, shown in Figure 1 by solid lines, and are indicative of relatively modest variances, and thus well-

defined straight lines. Figure 1 shows that the major rock-forming elements (Fe–Mg–Si) of individual chondrites within a particular class of chondrites are related in a relatively simple way, as indicated by the fact that data-points for members of the respective classes scatter about well-defined straight lines. For ordinary chondrite formation, two interpretations are possible: (1) the traditional one-component system and (2) the two-component system presented here.

One-component system: For decades, without the benefit of the well-defined straight-line relationship shown in Figure 1, differences in major element compositions of ordinary chondrites have been ascribed to ‘metal-silicate fractionation’^{15,20,21}. According to this view, points that lie along the ordinary chondrite line of Figure 1 may be considered as the result of simple addition or subtraction of iron metal from its parent material of unspecified origin. This view, however, does not explain in a logical,

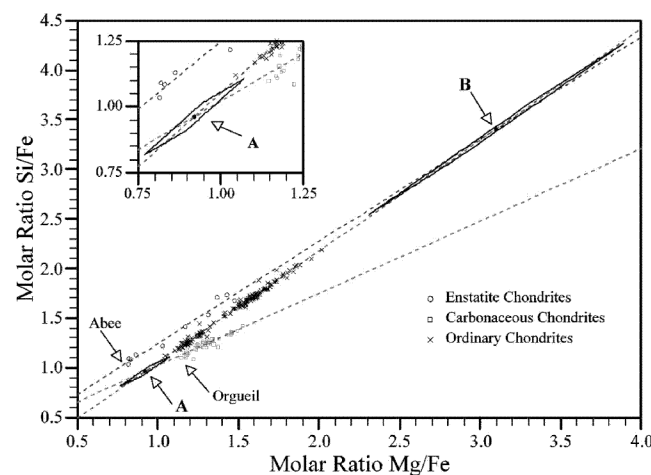


Figure 1. Molar (atom) ratios of Mg/Fe and Si/Fe from analytical data on 10 enstatite chondrites, 39 carbonaceous chondrites and 157 ordinary chondrites. Data from refs 9, 10 and 27. Members of each chondrite class dataset scatter about a unique, linear regression line indicated by dashes. Locations of the volatile-rich Orgueil carbonaceous chondrite and the volatile-rich Abee enstatite chondrite are indicated. Line intersections A and B are designated respectively as primitive and planetary components. Error estimates of points A and B are indicated by solid-line parallelograms formed from the intersections of the standard errors of the respective linear regression lines. (Inset) Standard error parallelogram of point A shown in expanded detail.

Table 1. Square of the correlation coefficient of each of the least squares fit lines for data of Figure 1 as ratios relative to iron, silicon and magnesium. Note that three well-defined lines occur only in the case of ratios with respect to iron

	Coordinates		
	(Mg/Fe, Si/Fe)	(Mg/Si, Fe/Si)	(Si/Mg, Fe/Mg)
Enstatite chondrite line	0.973	0.505	0.663
Ordinary chondrite line	0.990	0.264	0.175
Carbonaceous chondrite line	0.814	0.005	0.250

and causally related manner, their ubiquitous, systematic depletion of refractory siderophile elements.

Two-component system: The well-defined straight-line relationship shown in Figure 1 admits a different interpretation of ordinary chondrite formation as the result of mixing from two distinct reservoirs. Significantly, in Figure 1 the ordinary chondrite line intersects both the enstatite chondrite line and the carbonaceous chondrite line in the manner shown. As a consequence, data for the three major elements (Fe, Mg and Si) of each ordinary chondrite can be interpreted as lying along a mixing line and consisting of a mixture of two components. One component is defined by the intersection of the ordinary chondrite line and the carbonaceous chondrite line, designated A in Figure 1 and called primitive. The other component is defined by the intersection of the ordinary chondrite line and the enstatite chondrite line, designated B in Figure 1 and called planetary. Elements of the primitive source were not previously separated from one another appreciably, like the Orgueil chondrite, whereas the planetary source had previously suffered loss of iron metal from a different primitive-like parent matter, presumably during proto-planetary core-formation. An important distinction in the two-component system is that the loss of iron metal occurs not in the case of each ordinary chondrite separately, but in the planetary reservoir component prior to and perhaps in a different region of space from the loca-

tion of ordinary chondrite parent formation. In other words, differences in compositions of individual ordinary chondrites result primarily as a consequence of being formed from different proportions of their two parent components, defined here as primitive and planetary. One should note that the nomenclature employed here should not be confused with similar terms utilized in the literature, perhaps with somewhat different meanings.

The Mg/Fe and Si/Fe ratios of the primitive component can be read from the intersections of the straight lines in Figure 1 or by simultaneous solution of equations for the carbonaceous and ordinary chondrite straight lines with slopes and y-intercepts determined from the least squares fit:

$$\text{Primitive [Mg/Fe, Si/Fe]} = [0.9200, 0.9622]. \quad (1)$$

Similarly, the Mg/Fe and Si/Fe ratios of the planetary component can be read from line intersections in Figure 1 or by simultaneous solution of equations for the enstatite and ordinary chondrite straight lines with their respective slopes and y-intercepts:

$$\text{Planetary [Mg/Fe, Si/Fe]} = [3.0956, 3.4041]. \quad (2)$$

Any representative ordinary chondrite can be represented as a mixture of the primitive and the planetary compo-

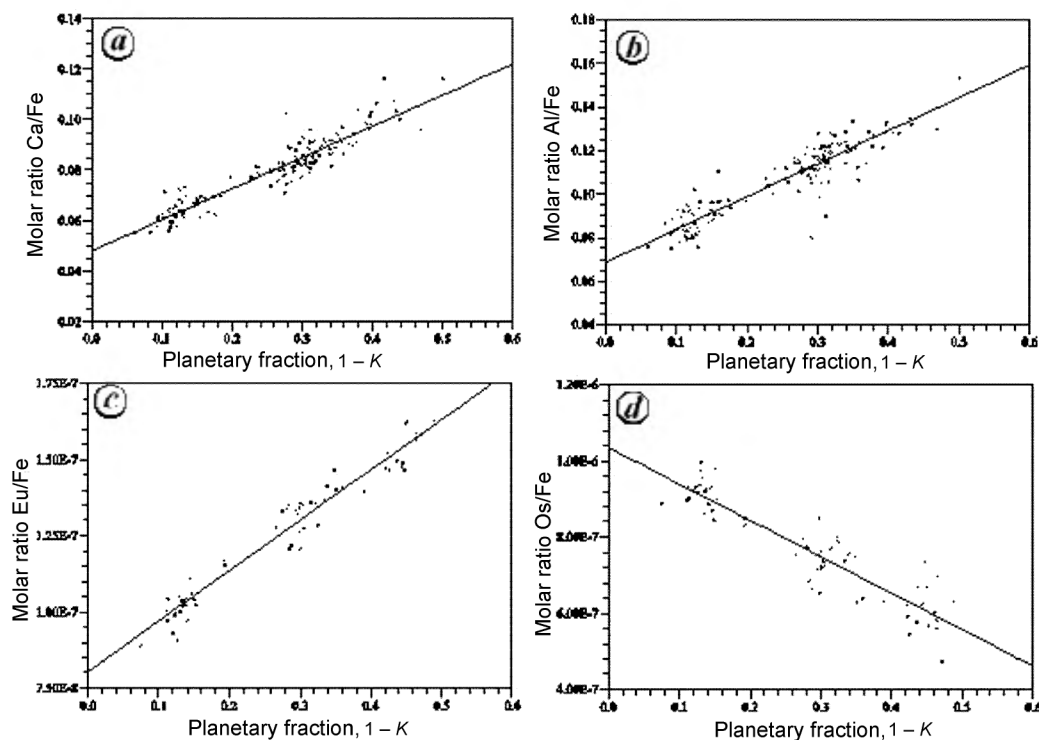


Figure 2. Examples of ordinary chondrite whole-rock molar (atom) ratios of elements relative to iron as a function of the planetary fraction. The square of the correlation coefficient for each of the linear regression lines is as follows: (a) Ca, 0.886; (b) Al, 0.845; (c) Eu, 0.954; (d) Os, 0.846. From analytical data of (Ca and Al)⁹ and (Eu and Os)²⁰.

nents. Using eqs (1) and (2) and defining the primitive fraction as K and the planetary fraction as $(1 - K)$, the molar Mg/Fe ratio of any ordinary chondrite is

$$[\text{Mg/Fe}] = 0.9200K + 3.0956(1 - K). \quad (3)$$

Similarly,

$$[\text{Si/Fe}] = 0.9622K + 3.4041(1 - K). \quad (4)$$

The value of K calculated for any particular ordinary chondrite from the ratio $[\text{Mg/Fe}]$ differs only by a small amount from the corresponding value of K calculated using the ratio $[\text{Si/Fe}]$. With the intent of smoothing analytical fluctuation, an average of the two values was assigned as the primitive fraction K of each ordinary chondrite; the planetary fraction being $(1 - K)$.

The above approach is justified for the special case of Figure 1 because Fe, Mg and Si (together with combined O and S) account for at least 95% of the mass of each chondrite and are fully condensable over a wide variety of conditions. Minor and trace element compositions of the primitive and planetary components cannot be obtained in the same manner, but estimates can be derived from correlations, provided the elements are fully condensable and are not readily exchanged with an ambient gas phase.

Ordinary chondrite analytical data for many minor and trace elements appear to correlate or to anti-correlate with the planetary fraction as shown in Figure 2. Estimates of the ratio E_i/Fe of the primitive and planetary components, obtained from the linear least squares regression line of the ordinary chondrite data as in the examples of Figure 2 are given in Tables 2 and 3.

The planetary component relative to iron is enriched approximately threefold in magnesium and silicon compared to the primitive component. Such enrichment in silicate-forming elements suggests that the planetary component is derived from the outer regions of a partially differentiated proto-planet. For the planetary component,

one might anticipate similar enrichment in other silicate-forming elements with corresponding deficiencies for iron and for the siderophile elements that dissolve in iron metal (Tables 2 and 3).

The approximately sevenfold greater depletion within the planetary component of refractory siderophile elements (Ir and Os) than other more volatile siderophile elements (Ni, Co and Au) indicates, in at least one instance, that planetary-scale differentiation and/or accretion progressed in a heterogeneous manner. The idea of heterogeneous proto-planetary differentiation and/or accretion is not new. For example, Eucken²² suggested core formation in the terrestrial planets as a consequence of successive condensation on the basis of relative volatility from a hot, gaseous proto-planet, with iron metal raining out at the centre. Turekian and Clark²³ reiterated the idea of heterogeneous accretion in the context of a lower pressure, lower temperature model.

There are reasons to associate the highly reduced matter of enstatite chondrites with the inner regions of the solar system: (1) The regolith of Mercury appears from reflectance spectrophotometric investigations²⁴ to be virtually devoid of FeO, like silicates of enstatite chondrites (and unlike silicates of other types of chondrites); (2) E-type asteroids (on the basis of reflectance spectra, polarization and albedo), the presumed source of enstatite meteorites, are, radially from the Sun, the innermost of the asteroids²⁵; (3) Only the enstatite chondrites and related enstatite achondrites have oxygen isotopic compositions indistinguishable from those of the earth and the moon¹⁴, and (4) Fundamental mass ratios of major parts of the earth (geophysically determined) are virtually identical to corresponding (mineralogically determined) parts of certain enstatite chondrites, especially the Abee enstatite chondrite^{5,6,12}.

The high bulk density of Mercury indicates that much of the silicate matter for the upper portion of its mantle was lost at some previous time¹⁻³. I suggest that some matter from the proto-planet of Mercury became the

Table 2. Estimates of elemental (molar) abundance ratios of the primitive and planetary components of ordinary chondrites for all applicable elements available from the data of Jarosewich⁹. For convenience, the square of the correlation coefficient for the relevant linear least squares regression line is shown in parenthesis. For comparison, corresponding elemental abundance ratios are shown for the Orgueil carbonaceous chondrite and the Abee enstatite chondrite

Element ratio	Planetary component B	Primitive component A	Ratio B/A	Orgueil chondrite	Abee chondrite
Mg/Fe (0.997)	3.0914	0.9217	3.35	1.19	0.82
Si/Fe (0.997)	3.4086	0.9609	3.55	1.08	1.11
Ca/Fe (0.886)	0.1715	0.0480	3.57	0.0802	0.0385
Al/Fe (0.845)	0.2197	0.0686	3.20	0.0956	0.0522
Ni/Fe (0.324)	0.0264	0.0648	0.41	0.0562	0.0566
Ti/Fe (0.629)	0.0074	0.0023	3.22	0.0018	0.0014
Mn/Fe (0.807)	0.0237	0.0070	3.39	0.0140	0.0117
Na/Fe (0.630)	0.1562	0.0400	3.91	0.0673	0.0668
Cr/Fe (0.755)	0.0331	0.0113	2.93	0.0105	0.0075
Co/Fe (0.073)	0.0017	0.0029	0.59	0.0027	0.0026
K/Fe (0.452)	0.0112	0.0031	3.61	0.0045	0.0039

Table 3. Estimates of elemental (molar) abundance ratios of the primitive and planetary components of ordinary chondrites for applicable trace elements from the data of Kallemeyn *et al.*²⁰. The planetary fraction of each chondrite is calculated from the equation of line intersection, obtained from Figure 1, using the individual ordinary chondrite molar Mg/Fe ratio. For convenience, the square of the correlation coefficient for the relevant linear least squares regression line is shown in parenthesis. For comparison, corresponding elemental abundance ratios are shown for the Orgueil carbonaceous chondrite and the Abee-like Kota–Kota enstatite chondrite from the data of Kallemeyn and Wasson²⁸. Kota–Kota data are used here because Abee was not included in this analytical suite

Element ratio	Planetary component B	Primitive component A	Ratio B/A	Orgueil chondrite	Abee-like Kota–Kota chondrite
Sc/Fe (0.958)	9.235E–05	2.823E–05	3.27	3.944E–05	2.466E–05
V/Fe (0.973)	7.373E–04	2.341E–04	3.15	3.415E–04	2.087E–04
Zn/Fe (0.763)	3.549E–04	1.171E–04	3.03	1.475E–03	8.447E–04
Ga/Fe (0.784)	3.264E–05	1.525E–05	2.14	4.332E–05	4.627E–05
La/Fe (0.936)	1.142E–06	3.490E–07	3.27	5.053E–07	3.499E–07
Sm/Fe (0.941)	6.442E–07	2.058E–07	3.13	2.780E–07	1.678E–07
Eu/Fe (0.954)	2.459E–07	8.055E–08	3.05	1.165E–07	6.806E–08
Yb/Fe (0.955)	6.506E–07	1.891E–07	3.44	2.945E–07	1.793E–07
Lu/Fe (0.958)	9.219E–08	2.954E–08	3.12	4.186E–08	2.483E–08
Au/Fe (0.733)	1.212E–07	2.443E–07	0.50	2.386E–07	3.182E–07
Os/Fe (0.846)	8.090E–08	1.035E–06	0.078	7.862E–07	6.851E–07
Ir/Fe (0.838)	6.567E–08	9.575E–07	0.069	7.240E–07	6.058E–07

planetary component of the ordinary chondrites, presumably separated at the time of the core formation of Mercury through dynamic instability and/or expulsion during the sun's initially violent ignition and approach toward thermonuclear equilibrium.

The planetary component of the ordinary chondrites lies along the differentiated portion of the enstatite chondrite line in Figure 1 and is therefore expected to be highly reduced, like Mercury²⁴. Moreover, despite great uncertainties, the relative masses involved are all consistent with the possibility that the complement of lost elements of Mercury became the planetary component of ordinary chondrite formation, re-evaporated together with a more oxidized component of primitive matter, ending up mainly in the region of the asteroid belt, the presumed source region for the ordinary chondrites. Such a picture would seem to explain for the ordinary chondrites, their major element compositions, their intermediate states of oxidation, and their ubiquitous deficiencies of refractory siderophile elements.

On the supposition that the complement of lost elements of Mercury is in fact identical to the planetary component of ordinary chondrite formation, I have estimated, as a function of the core mass of Mercury, the total mass of ordinary chondrite matter originally present in the solar system. Although the mass of Mercury is well known, its moment of inertia, and hence its core mass are not. For a core mass of 75%, the calculated total mass of ordinary chondrite matter originally present in the solar system amounts to 1.83×10^{24} kg, about 5.5 times the mass of Mercury²⁶. That amount of mass is insufficient to have formed a planet as massive as the earth, but may have contributed significantly to the formation of Mars, as well as adding to the veneer of other planets, including earth. Presently, only about 0.1% of that mass remains in the asteroid belt.

1. Urey, H. C., The origin and development of the Earth and other terrestrial planets. *Geochim. Cosmochim. Acta*, 1951, **1**, 36–82.
2. Urey, H. C., *The Planets*, Yale University Press, New Haven, 1952.
3. Bullen, K. E., Cores of terrestrial planets. *Nature*, 1952, **170**, 363–364.
4. Chapman, C. R., *Mercury* (eds Vilas, F., Chapman, C. R. and Mathews, M. S.), University of Arizona Press, 1988, pp. 1–23.
5. Herndon, J. M., The chemical composition of the interior shells of the Earth. *Proc. R. Soc. London, Ser. A*, 1980, **372**, 149–154.
6. Herndon, J. M., Feasibility of a nuclear fission reactor at the center of the Earth as the energy source for the geomagnetic field. *J. Geomagn. Geoelectr.*, 1993, **45**, 423–437.
7. Daly, R. A., Meteorites and an earth model. *Bull. Geol. Soc. Am.*, 1943, **54**, 401–456.
8. Meunier, M. S., Structure du globe d'où proviennent les météorites. *Compt. Rend.*, 1871, **72**, 111–113.
9. Jarosewich, E., Chemical analyses of meteorites: A compilation of stony and iron meteorite analyses. *Meteoritics*, 1990, **25**, 323–337.
10. Wiik, H. B., On regular discontinuities in the composition of meteorites. *Commentat. Phys.-Math., Soc. Sci. Fenn.*, 1969, **34**, 135–145.
11. Urey, H. C. and Craig, H., The composition of stone meteorites and the origin of the meteorites. *Geochim. Cosmochim. Acta*, 1953, **4**, 36–82.
12. Herndon, J. M., Sub-structure of the inner core of the earth. *Proc. Natl. Acad. Sci. USA*, 1996, **93**, 646–648.
13. Mason, B., The classification of chondritic meteorites. *Am. Mus. Novit.*, 1962, **2085**, 1–20.
14. Clayton, R. N., Oxygen isotopes in meteorites. *Annu. Rev. Earth Planet. Sci.*, 1993, **21**, 115–149.
15. Larimer, J. W., Chemical fractionation in meteorites I. Condensation of the elements. *Geochim. Cosmochim. Acta*, 1967, **31**, 1215–1238.
16. Herndon, J. M. and Suess, H. E., Can the ordinary chondrites have condensed from a gas phase? *Geochim. Cosmochim. Acta*, 1977, **41**, 233–236.
17. Herndon, J. M., Reevaporation of condensed matter during the formation of the solar system. *Proc. R. Soc. London, Ser. A*, 1978, **363**, 283–288.
18. Scott, E. R. D., Chondrites and the protoplanetary disk. *Annu. Rev. Earth Planet. Sci.*, 2007, **35**, 577–620.

19. Marhas, K. K. and Goswami, J. N., Boron isotopic composition in early solar system solids: An ion microprobe study. *Curr. Sci.*, 2000, **78**, 78–81.
20. Kallemeyn, G. W. *et al.*, Ordinary chondrites: Bulk compositions, classification, lithophile-element fractionations, and composition-petrographic type relationships. *Geochim. Cosmochim. Acta*, 1989, **53**, 2747–2767.
21. Ahrens, L. H., Si–Mg fractionation in chondrites. *Geochim. Cosmochim. Acta*, 1964, **28**, 411–423.
22. Eucken, A., Physikalisch-chemische Betrachtungen ueber die fruehste Entwicklungsgeschichte der Erde. *Nachr. Akad. Wiss. Goettingen, Math.-Phys. Kl.*, 2, 1944, 1–25.
23. Turekian, K. K. and Clark, S. P., Inhomogeneous accumulation of the earth from the primitive solar nebula. *Earth Planet. Sci. Lett.*, 1969, **6**, 346–348.
24. Vilas, F., Mercury: Absence of crystalline Fe²⁺ in the regolith. *Icarus*, 1985, **64**, 133–138.
25. Zellner, B. *et al.*, The E asteroids and the origin of the enstatite achondrites. *Geochim. Cosmochim. Acta*, 1977, **41**, 1759–1767.
26. Herndon, J. M., Total mass of ordinary chondrite material originally present in the Solar System. ArXiv: astro-ph/0410242, 2004.
27. Baedecker, P. A. and Wasson, J. T., Elemental fractionations among enstatite chondrites. *Geochim. Cosmochim. Acta*, 1975, **39**, 735–765.
28. Kallemeyn, G. W. and Wasson, J. T., The compositional composition of chondrites-I. The carbonaceous chondrite groups. *Geochim. Cosmochim. Acta*, 1981, **45**, 1217–1230.

Received 9 February 2007; revised accepted 18 May 2007

Impact of Indonesian throughflow blockage on the Southern Indian Ocean

Vivek Kumar Pandey*, Vihang Bhatt, A. C. Pandey and I. M. L. Das

K. Banerjee Centre of Atmospheric and Ocean Studies, Institute of Inter-Disciplinary Studies, University of Allahabad, Allahabad 211 002, India

The present study deals with the numerical simulation of the Indonesian throughflow (ITF) via three major passages, namely Lombok strait (115°E, 8°S), Savu strait (122°E, 9°S) and Timor strait (128°E, 11°S), its seasonal variability and impact on the sea surface parameters due to its blockage. The model is initialized with the Levitus94 climatological dataset for annual mean temperature and salinity fields, and is forced by the seasonal and yearly varying da Silva SMD 1994 and Hellerman and Rosenstein wind datasets. The spin-up of the model has been carried out separately for open and closed Indonesian channels using both the surface wind climatologies. Numerical simulations confirm that the ITF is mainly towards Indian Ocean in a year. It has been observed that surface winds have an impact on the phase as well as magnitude of the ITF. The net effect of blockage is reduction in

temperature of the Southern Indian Ocean and no significant change is seen in surface salinity.

Keywords: Blockage, Indonesian throughflow, passages, Southern Indian Ocean.

THE Indonesian throughflow (ITF) has long been a focus of research interest due to its impact on regional and global ocean circulation, both in modern and past time periods^{1–3}. The ITF refers to the exchange of water and heat between the Indian Ocean (IO) and Pacific Ocean basins. It transfers warm, low-salinity waters from the western Pacific into the IO from where the Asian monsoon gathers strength. As an integral element of the global ocean circulation, it is influential in regulating climate and rainfall across Indonesia, India and Australia. The Indonesian Archipelago region has three major conduits for inter-ocean tropical thermocline water from the Pacific Ocean to the IO⁴, namely Lombok strait (115°E, 8°S), Savu strait (122°E, 9°S) and Timor passage (128°E, 11°S).

The ITF is governed by Pacific Ocean to IO pressure gradient with strong seasonal and interannual variability^{5,6}. The primary path of the ITF is through the Makassar strait^{7,8}. The throughflow is high during June–August (southeast monsoon) and low during December–February (northeast monsoon)⁵. During June–August, surface water is driven from Banda Sea into Floras, Java and South China seas, whereas during December–February, surface water from Java Sea and Makassar strait is driven across Floras Sea into Banda Sea⁹. Observations and model studies suggest that the ITF transport varies by as large as ± 4 Sv (1 Sv = 10^6 m³/s) with the phase of El Nino- Southern Oscillation (ENSO) (maximum ITF transport during La-Nina and minimum during El Nino)¹⁰ and lags the ENSO cycle by 8–9 months¹¹.

In a unique study using a coupled ocean–atmosphere model, Schneider¹² has shown the effect of ITF on the oceanic circulation and thermocline depth in the IO and around Australia. This study shows that the ITF increases the surface temperature in the eastern IO. It also reduces surface temperatures in the equatorial Pacific Ocean and shifts the warm pool towards west, i.e. eastern IO. This self-control on the sea-surface temperature affects the atmospheric pressure in the entire tropics and mid-latitudes via atmospheric tele-connections. Numerical simulations also suggested that the ITF transport significantly contributes to the Eastern IO circulation¹³. The magnitude and variability of the Pacific and Indian Ocean (PACIO) throughflow for accurate determination of the mass, heat and salt fluxes in the PACIO region was also emphasized earlier^{6,14,15}. Godfrey¹⁶ discussed several aspects of ITF effects on the PACIO circulation and its impact on the surface heat flux of the IO.

The present study aims to carry out sensitivity studies with the Princeton Ocean Model (POM) to see the impact of ITF on the dynamics of the Southern Indian Ocean (SIO) and variability of the ITF.

*For correspondence. (e-mail: vivekvpandey@rediffmail.com)